

indicate that the motional states of species A and B do not depend appreciably on Si/Al, at least in the range $34 \leq \text{Si/Al} \leq 120$.

The strength and number of acid sites in a zeolite depend on the concentration of tetrahedral aluminum atoms²¹ and their locations in the pore structure.²² For a highly dealuminated zeolite ZSM-5 such as sample 490, aluminum sites will generally be limited in number and methoxyl groups bound to silanol groups will have local structural and dynamic environments substantially different from that of a similar group adsorbed in H-ZSM-5 with a lower Si/Al ratio, in which case interactions with nearby aluminum centers is possible. The temperature dependence of the relaxation of species C (Figure 5) is like that of a spin relaxing through dipole-dipole coupling when $\omega_0\tau_c \ll 1$:

$$\ln T_{1,DD} = \ln K - \frac{E_a}{RT} \quad (11)$$

The slope of the line in Figure 5 gives an activation energy of $2.07 (\pm 0.15)$ kcal/mol, a very low activation energy compared to the activation energy of species B, which is also bound. Thus, species C must have more rotational freedom, because of (1) lack of direct interactions (e.g., with aluminum centers) that limit its rotational mobility at the site or (2) more facile exchange with the mobile physisorbed phase resulting in an average relaxation rate shorter than that of species B or (3) because both of these mechanisms are active. Clearly, species C is, in either case, more mobile than species B.

Conclusions

The ¹³C NMR measurements of spin-dynamic parameters for the methanol/H-ZSM-5 system give information about molecular rotational mobility of three different sorbed species. Physisorbed methanol (A), most likely a mobile species in the channels of the ZSM-5 zeolite, has a rather short spin-lattice relaxation time, the temperature dependence of which can be ascribed to relaxation by spin-rotation coupling. Species B behaves as if it moves anisotropically, and it has the highest energy of activation—in the range 9–11 kcal/mol. We attribute this species to methanol chemisorbed at Brønsted sites in H-ZSM-5 with Si/Al < 120. The third species (C), existing only in sample 490, has a shorter relaxation time than species B under similar conditions. In this sample, the dominant characteristic is the much lower concen-

tration of aluminum in the framework. Methoxyl groups bound to silanols in this material have a much lower probability of interacting strongly with an aluminum center than do methoxyl groups in samples of lower Si/Al ratio. The reorientation activation energy and magnitude of the relaxation time of species C clearly show that this species has more rotational mobility than does species B. One can rationalize this result if species C is subject to fewer direct interactions with aluminum centers that restrict rotational mobility or if exchange causes more efficient relaxation.

In the cases where we observe species B (samples 34, 67, and 120), the reorientation activation energy of the motion that induces spin-lattice relaxation does not seem to depend strongly on the Si/Al ratio. Therefore, we conclude that the local environments of the bound methoxyl groups in these three materials are quite similar and allow less rotational mobility than in the highly siliceous material. Species A, which is present in all samples we investigated, has spin-lattice relaxation parameters that are independent of the Si/Al ratio, a fact consistent with the assignment of this species to physisorbed methanol.

Subjecting methanol-containing zeolites to temperatures between 295 and 473 K for short times results only in the conversion of methanol to dimethyl ether. The material with a Si/Al ratio of 490 is essentially inactive for this conversion, even at 473 K. Under the conditions of treatment in these experiments, we detect no subsequent products over any of the four catalysts.^{3,4} Thus, the conversion to dimethyl ether is extremely facile over materials of sufficiently low Si/Al ratio, but the subsequent steps in the methanol to hydrocarbon conversion over H-ZSM-5 require a higher temperature to activate secondary reactions. Since this conversion only occurs for samples in which species B is present (samples 34, 67, and 120), we conclude that this species, which we have assigned as a methoxysilane group interacting with a Brønsted site, is the precursor that ultimately leads to production of hydrocarbons over this catalyst.

Acknowledgment. This work was supported by the donors of the Petroleum Research Fund, administered by the American Chemical Society, and the Sponsors of the Center for Catalytic Science and Technology of the University of Delaware. C.T. acknowledges a Sun fellowship during part of this work. We acknowledge Professor J. H. Noggle for useful discussions and R. W. Nickle (deceased) and J. H. McCartney for technical assistance.

Registry No. CH₃OH, 67-56-1.

(21) Jacobs, P. A. *Carboniogenic Activity of Zeolites*; Elsevier: Amsterdam, 1977.

(22) Derouane, E. G.; Vadrine, J. C. *J. Mol. Catal.* **1980**, *4*, 479.

Comparison of Free Energy Changes for Nitrogen Inversion and Electron Loss. 3. 9-Halo-9-azabicyclo[3.3.1]nonanes

Stephen F. Nelsen,* Peter A. Petillo, and Daniel T. Rumack

Contribution from the Department of Chemistry, University of Wisconsin, Madison, Wisconsin 53706. Received December 29, 1989

Abstract: The nitrogen inversion barrier for 1-Br was measured by dynamic ¹³C NMR between -11 and +54 °C to be $\Delta G^\ddagger(25^\circ\text{C}) = 13.75 \pm 0.09$ kcal/mol, $E^\circ(\text{CH}_3\text{CN}/0.1 \text{ M Bu}_4\text{NClO}_4, \text{ vs SCE}) = +1.37 \text{ V}$, and $v\text{IP} = 8.30 \text{ eV}$. For 1-I, the corresponding numbers are $\Delta G^\ddagger(-93^\circ\text{C})$ estimated at 7.5 kcal/mole by the T_c method, $E^\circ = +1.12 \text{ V}$, $v\text{IP} = 8.07 \text{ eV}$. These numbers are compared with those for 1-Cl, 1-O[•], 1-*t*-Bu, and 1-Me, as well as with semiempirical AM1 calculations. When separated from nitrogen pyramidalization effects, changes in ease of electron removal in solution for this series of 1-X compounds relative to 1-Cl are about 18 to 60% of those observed for vertical ionization in the gas phase.

Introduction

N-substituted cyclic and bicyclic dialkylamines of general formula R₂NX exhibit parallel behavior between their thermodynamics for cation radical formation and kinetics for nitrogen atom inversion.¹ Changes in alkyl group structure that cause

more difficult electron removal also raise the nitrogen inversion barrier for the neutral compound. The reason for this coupling

(1) (a) Nelson, S. F.; Cunkle, G. T.; Gannett, P. M.; Ippoliti, J. T.; Qualy, R. J. *J. Am. Chem. Soc.* **1983**, *105*, 3119. (b) Nelson, S. F.; Blackstock, S. C.; Steffek, D. J.; Cunkle, G. T.; Kurtzweil M. L. *Ibid.* **1988**, *110*, 6149.

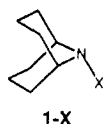
Table I. ^{13}C NMR Chemical shifts (δ) for Halogen Derivatives of 1

compd (T, °C)	C ₃ ,C ₇	C _{2,4(ayn)}	C _{6,8(anti)}	C _{1,5}
1-F ^a (+39)	18.85 (J = 1.5)	22.50 (J = 8.0)	31.86 (J = 12.3)	56.67 (J = 7.0)
1-Cl ^b (-17)	19.51, 20.14 (+54)	23.08 28.53	33.58 28.53	59.69 59.96
1-Br ^c (+7)	19.61 (+54)	24.83 29.07	33.07 29.07	60.98 61.16
1-I ^d (+11)	20.69	30.26	30.26	62.70

^a In CDCl₃. All peaks were doublets, caused by long-range ^{13}C - ^{19}F coupling, quoted in Hz. ^b In CDCl₃, from ref 1a. ^c In CDCl₃. ^d In CD₂Cl₂.

of two processes that initially appear to be quite different in that flattening at nitrogen occurs during both of them.

The 9-azabicyclo[3.3.1]nonyl group provides substantial "Bredt's rule" kinetic stabilization for its radical cations.² Overlap of the C_α-H bonds with the formally singly occupied π -rich orbital at N₉ of the radical cation is severely restricted geometrically, which increases radical cation lifetime so much that the thermodynamically significant formal potential for oxidation, $E^{\circ'}$, proved measurable for 1-Cl despite the difficulty of its oxidation.² In this work we explore the relationship between nitrogen inversion barrier and ease of electron loss for haloamines 1-X, where X =



F, Cl, Br, and I. Loss of HX is especially rapid for the compounds at the ends of this series, making even characterization of fluoroamines and iodoamines with the C_α-H bond difficult in most cases. Formation of an untwisted C=N bond from 1-X is impossible, inhibiting loss of HX.

Results

N Inversion Barrier, CV, and PE of 1-X. 1-Br and 1-I were prepared by reaction of 1-H•HCl with the *N*-halosuccinimides, and 1-F by its reaction with FClO₃, as described in the Experimental Section. The ^1H NMR spectra of these haloamines are complex and overlapping, and their ^{13}C NMR spectra are much easier to interpret. The chemical shifts observed are summarized in Table I. 1-F decomposed at +65 °C, before any effects of nitrogen inversion were observed on its NMR spectrum. The N inversion barrier for 1-Br was determined by dynamic ^{13}C NMR. Rate constants determined by digital simulation at nine temperatures between -11 and +54 °C were fit to an Eyring plot, giving $\Delta G_i^\ddagger(25^\circ\text{C}) = 13.75 \pm 0.09$ kcal/mol, $\Delta H_i^\ddagger = 11.8 \pm 1.3$ kcal/mol, and $\Delta S_i^\ddagger = -6.4 \pm 4.3$ eu, which should be compared with the barriers previously determined by the same method for 1-Cl of $\Delta G_i^\ddagger(25^\circ\text{C}) = 14.26 \pm 0.05$ kcal/mol, $\Delta H_i^\ddagger = 14.8 \pm 0.5$ kcal/mol, and $\Delta S_i^\ddagger = 1.7 \pm 1.8$ eu.^{1a} We were unable to observe any effects caused by slowing nitrogen inversion for 1-I down to -84 °C at 25.16 MHz, but at higher field, we observed T_c of -93 ± 2 °C at 125.12 MHz. Solubility problems prevented us from going to a low enough temperature to measure $\Delta\nu$ for the slow exchange limit spectrum directly, but the $\Delta\delta$ values observed for the F, Cl, and Br compounds give $\Delta\nu$ values of 1171, 1374, and 1031 Hz, leading to an estimation of $\Delta G_i^\ddagger = 7.5 \pm 0.05$ kcal/mol at -93 °C for 1-I. The actual uncertainty in ΔG_i^\ddagger is larger, and we quote 0.5 kcal/mol for the extrapolation to 25 °C in Table II.

Reversible cyclic voltammetry curves were observed for 1-Br and 1-I, but unfortunately 1-F showed only an irreversible oxidation wave, indicating a short lifetime for the cation radical of this very difficultly oxidized compound. We were also unsuccessful in seeing any reversibility in the CV curve of 1-F at -78 °C in butyronitrile containing 0.1 M tetra-*n*-butylammonium perchlorate, observing a peak potential of 2.37 V vs SCE at 0.2 V/s

Table II. Experimental Nitrogen Inversion and Oxidation Data for Derivatives of 1

	1-F	1-Cl	1-Br	1-I
$\Delta G_i^\ddagger(25^\circ\text{C})^a$, kcal/mol		14.3	13.8	$\sim 7.8 \pm 0.5$
$\delta\Delta G_i^\ddagger,^b$ kcal/mol		[0]	-0.5	~ -6.5
$E^{\circ'},^c$ V	ir 2.0 ^d	1.49	1.37	1.12
$\delta\Delta G_i^{\circ'},^e$ kcal/mol	[+11.5]	[0]	-2.8	-8.5
$\nu\text{IP},^f$ eV		8.55	8.30	8.07
$\delta\nu\text{IP},^g$ kcal/mol		[0]	-5.8	-11.1

^a Measured by dynamic NMR. ^b $\delta\Delta G_i^\ddagger = \Delta G_i^\ddagger(1-X) - \Delta G_i^\ddagger(1-Cl)$. ^c Measured by cyclic voltammetry. Conditions: CH₃CN containing 0.1 M tetra-*n*-butylammonium perchlorate, versus SCE, at Pt. ^d Irreversible oxidation wave observed. Peak potential at 0.2 V/s scan rate reported. ^e From eq 1. ^f Measured by photoelectron spectroscopy. ^g From eq 2.

Table III. AM1 Calculations on Halogenated Derivatives of 1

	1-F	1-Cl	1-Br	1-I
optimized neutral				
ΔH_f , kcal/mol	-22.1	-2.8	+7.8	+14.1
$\alpha(\text{av})^a$, deg	109.6	110.4	111.9	113.0
optimized cation radical				
ΔH_f^b , kcal/mol	172.6	186.7	194.0	198.0
other calculated quantities				
ΔH_f^c , kcal/mol	17.0	13.6	8.0	4.5
$\nu\text{IP},^d$ eV	9.09	8.90	8.63	8.44
$\Delta H_{rc},^e$ kcal/mol	14.8	15.6	12.8	10.7 ^b
$a\text{IP},^f$ kcal/mol	194.8	189.6	186.2	183.9
changes as halogens are changed				
$\delta\nu\text{IP},^g$ kcal/mol	+4.4	[0]	-6.2	-10.6
$\delta a\text{IP},^h$ kcal/mol	+5.2	[0]	-3.4	-5.7
$\delta\Delta H_f^i$, kcal/mol	+3.4	[0]	-5.6	-9.1
$\delta\Delta H_f^j$, kcal/mol	+1.7	[0]	+2.2	+3.4

^a Average of heavy atom bond angles at N. ^b AM1-UHF for the radical cations. ^c $\Delta H_f(\text{neutral optimized with planar nitrogen atom}) - \Delta H_f(\text{neutral})$. ^d $\Delta H_f(\text{cation optimized with planar nitrogen atom}) - \Delta H_f(\text{cation})$. ^e $\Delta H_f(\text{cation}) - \Delta H_f(\text{neutral})$. ^f $a\text{IP}(1-X) - a\text{IP}(1-Cl)$. ^g $\Delta H_f^c(\text{cation}) - \Delta H_f^c(\text{neutral optimized with planar nitrogen atom})$. ^h $\Delta H_f^c(\text{cation}) - \Delta H_f^c(\text{neutral optimized with planar nitrogen atom})$. ⁱ $\delta\Delta H_f = [\Delta H_f^c(1-X) - \Delta H_f^c(1-Cl)]$.

scan rate and 2.31 V vs SCE at 0.02 V/s scan rate. The vertical ionization potentials for 1-Br and 1-I were determined by photoelectron (PE) spectroscopy, but 1-F proved to be too unstable for us to measure its PE spectrum.

The nitrogen inversion and oxidation data measured here are compared with those previously determined for 1-Cl in Table II, and changes in the measured quantities from those of 1-Cl are given in kcal/mol. Our experimental difficulties preclude conclusions about 1-F except that it is both slow to invert and difficult to oxidize relative to the other compounds.

Semiempirical MO Calculations. Semiempirical AM1 calculations³ have been carried out on the neutral and radical cation forms of these haloamines for comparison with experimental data, and the results are summarized in Table III. The AM1 calculations are far from perfect, but we believe that comparing the calculated results with available experiments is useful, both to see how successful the calculations are and to see whether they allow better understanding of changes in ease of ionization and of inversion barriers as the halogens are changed. As is typical for trisubstituted nitrogen compounds, the calculated νIP values are somewhat high, but their differences from the experimental values are 0.35 (1-Cl), 0.33 (1-Br), and 0.37 (1-I), which are constant to within the ~ 0.03 eV (~ 0.7 kcal/mol) error of the PE measurements. AM1 thus calculates the effect of changing halogens on νIP quite successfully. The nitrogen inversion barriers calculated by AM1 are also lower than the experimental values.⁴ The calculated ΔH_f^\ddagger for 1-Cl is about 1.2 kcal/mol below the

(3) Dewar, M. J. S.; Zoebisch, E. G.; Healy, E. F.; Stewart, J. J. P. *J. Am. Chem. Soc.* **1985**, *107*, 3902.

(4) For a comparison of the effect of changing alkyl groups on calculated and experimental barriers for N inversion in methylamines and chloroamines, see: Nelsen, S. F.; Ippoliti, J. T.; Frigo, T. B.; Petillo, P. A. *J. Am. Chem. Soc.* **1989**, *111*, 1776.

(2) Nelsen, S. F.; Kessel, C. R.; Brien, D. J. *J. Am. Chem. Soc.* **1980**, *102*, 702.

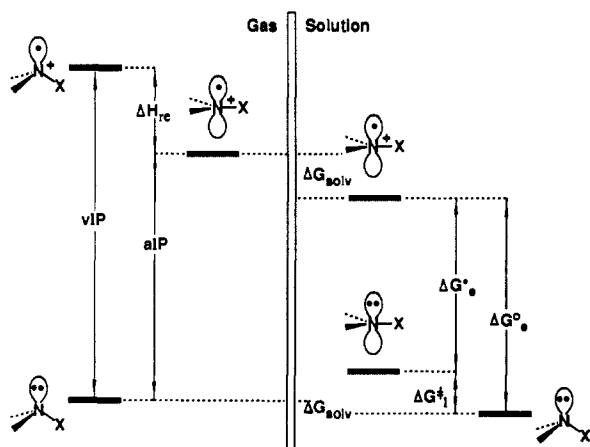


Figure 1. Diagrammatic comparison of gas- and solution-phase oxidation experiments for an R_2NX compound with pyramidal nitrogen in the neutral form and a planar nitrogen in the radical cation.

experimental value,^{1a} while those for **1-Br** and **1-I** are about 3.8 and 2.3 kcal/mol lower than the observed barriers. It will be noted from Table III that the calculated changes in nitrogen inversion barriers more closely parallel the changes in vIP than do the experimental results. AM1 calculations are far more successful than the newer parametrization, MNDO-PM3,⁵ which even gets the order for both nitrogen inversion barrier and for vIP as halogen is changed wrong, obtaining both quantities higher (2.0 kcal/mol and 0.14 eV, respectively) for **1-Br** than for **1-Cl**.

Discussion: Comparison of Nitrogen Inversion and Electron Removal Data

The energy diagram of Figure 1 summarizes the relationship between gas-phase ionization potential, solution-phase oxidation potential, and nitrogen inversion barrier. $E^{o'}$ is a relative measurement, not an absolute one like vIP , but changes in $E^{o'}$ are changes in the free energy for electron loss, ΔG_e^o . We choose to use **1-Cl** as the standard compound and discuss changes relative to the values for it in all cases. We use δ to indicate such changes. thus eq 1 gives the experimental changes in ease of electron loss

$$\delta\Delta G_e^o(\mathbf{1-X}) = 23.06[E^{o'}(\mathbf{1-X}) - E^{o'}(\mathbf{1-Cl})] \quad (1)$$

in kcal/mol, in solution. We note that photoelectron spectroscopy only directly measures vIP for compounds like the ones under discussion, which have a large geometry change upon electron loss so that vibrational fine structure is lost and the 0,0 band for ionization has vanishingly small intensity, and cannot be located. Equation 2 gives the experimental changes in gas-phase vIP , in kcal/mol. As shown in Table II, the experimental changes be-

$$\delta vIP(\mathbf{1-X}) = 23.06[vIP(\mathbf{1-X}) - vIP(\mathbf{1-Cl})] \quad (2)$$

tween the gas and solution phase ease of electron removal as the halogens are changed are rather different. δvIP being 2.08 times $\delta\Delta G_e^o$ for the bromide but 1.30 for the iodide.

We do not know how to predict the size of the change in ease of oxidation for **1** caused by the substitution of **Br** and **I** for **Cl** using substituent parameters. Both σ and σ_1 substituent parameters are virtually identical for **Cl** and **Br**, while **I** is somewhat less electron withdrawing in solution phase substituent parameter work.⁶ Although gas-phase ionization potentials for bromides and iodides are always lower than those for chlorides, the amount depends greatly upon to what the halide is attached. Eight simple alkyl bromides have a 0.65 ± 0.11 eV lower oxidation potential than the corresponding chlorides,⁷ while bromobenzene only has a 0.03 eV lower vIP than chlorobenzene,⁸ and the alkyl iodides

Table IV. Values of the Relative Ease of Oxidation of the Planar Forms of **1-X** Derivatives Estimated from Eq 4

X in 1-X	$\delta\Delta G_e^{o'a}$	$\delta\Delta G_i^{\ddagger a}$	$\delta\Delta G_e^{o'a}$	$\delta\Delta vIP^a$
[Cl]	[0]	[0]	[0]	[0]
Br	-2.8	-0.5	-2.3	-5.8
I	-8.5	~ -6.5	~ -2.0	-11.1
O [*]	-21.0	-13.3 ± 1^b	-7.7 ± 1	-26.7
<i>t</i> -Bu	-19.8	-13.3 ± 1^c	-9.5 ± 1	-28.8
Me	$\{-16.8\}^d$	-7.2 ± 0.3	$\{-9.6\}$	-16.4

^aUnit, kcal/mol. ^bAssuming a nitrogen inversion barrier of 2 kcal/mol or less for **1-O^{*}**. ^cAssuming ΔG_i^{\ddagger} for **1-t-Bu** is 4 ± 1 kcal/mol. ^dUsing E_p^{ox} instead of $E^{o'}$.

have 1.60 ± 0.14 eV lower oxidation potential than the chlorides,⁷ and iodobenzene a 0.27 eV lower oxidation potential than chlorobenzene.⁸ The differences in pyramidalities that are doubtless present for different **1-X** compounds are expected to affect both vertical and adiabatic ionization potentials, precluding accurate predictions by any empirical method we know that is based on substituent parameters for the halogen atoms. There is a significant correlation between $\delta\Delta vIP(\mathbf{1-X})$ and the electronegativity of the halogen atom. With use of Allen's new spectroscopically based electronegativities χ_{spec} ,⁹ the correlation coefficient for a plot of vIP versus χ_{spec} is 0.98 (deviations observed minus line are +0.75 kcal/mol for X = Cl, -1.2 kcal/mol for Br, +0.4 kcal/mol for I). We take this as evidence that there is little change in π stabilization energies of $(\mathbf{1-X})^{+\cdot}$ for these halogens. The correlation with electronegativity fails spectacularly for the related nitroxide, **1-O^{*}**, where a second-row atom is attached to the nitrogen. The correlation line gives $\delta\Delta vIP(\mathbf{1-O}^*)$ at +14.9 kcal/mol, but the observed $\delta\Delta vIP$ value is -26.7 kcal/mol (see Table IV below), so the nitroxide is 41.6 kcal/mol (1.8 eV) easier to oxidize than consideration of only the electronegativity of the atom attached to nitrogen predicts, presumably because of the large difference in π stabilization between the neutral and cationic forms.²

The change in formal oxidation potential as the halogen is changed, $\delta\Delta G_e^o$, can be broken up into changes in nitrogen inversion barrier, $\delta\Delta G_i^{\ddagger}$, and changes in the barrier to electron loss from the planar nitrogen transition state for inversion, $\delta\Delta G_e^{\ddagger}$, and changes in the barrier to electron loss from the planar nitrogen transition state for inversion, $\delta\Delta G_e^o$, as shown graphically in Figure 1 and numerically in eq 3. Although it might have been thought that the effect of changing halogen upon electron loss from the

$$\delta\Delta G_e^o = \delta\Delta G_i^{\ddagger} + \delta\Delta G_e^{\ddagger} \quad (3)$$

planar nitrogen form might be estimated from changes in the vertical ionization potential measured by PE spectroscopy, that is, that eq 4 might hold,

$$\delta\Delta G_e^o \approx \delta vIP \quad (4)$$

this is rather clearly not the case. Use of eq 4 with eq 3 to estimate $\delta\Delta G_i^{\ddagger}$ from the experimental $\delta\Delta G_e^o$ and δvIP numbers of Table IV gives $\delta\Delta G_i^{\ddagger}$ values of +2.9 (**1-Br**) and +2.6 (**1-I**) kcal/mol, while the experimental numbers are -0.5 (**1-Br**) and ca. -6.5 (**1-I**) kcal/mol. It has previously been shown for hydrazines that changes in vIP do not parallel changes in aIP as the structure of the alkyl groups is changed.¹⁰ Although the geometry change upon ionization is much simpler for **1-X** than for tetraalkylhydrazines because an N-halogen bond is cylindrically symmetrical, eq 4 clearly does not hold experimentally for **1-X** compounds either.

AM1 calculations predict the radical cations of all four **1** halides to be planar at nitrogen. Goldberg and co-workers¹¹ have shown

(8) (a) Potts, A. W.; Lyus, M. L.; Lee, E. P. F.; Fattahallah, G. H. *J. Chem. Soc. Faraday Trans. II* **1980**, *76*, 556. (b) For comparison, adiabatic IP values are 9.06 (PhCl), 8.98 (PhBr), 8.685 (PhI), and 8.56 (PhO^{*}); Lias, S. G.; Bartmess, J. E.; Liebman, J. F.; Holmes, J. L.; Levin, R. D.; Mallard, W. G. *Gas-Phase Ion and Neutral Thermodynamics*, *J. Phys. Chem. Ref. Data* **1988**, *17*, Supplement I.

(9) Allen, L. C. *J. Am. Chem. Soc.* **1989**, *111*, 9003.

(10) Nelsen, S. F.; Rumack, D. T.; Meot-Ner(Mautner), M. *J. Am. Chem. Soc.* **1988**, *110*, 7945.

(11) Goldberg, I. B.; Crowe, H. R.; Christe, K. O. *Inorg. Chem.* **1978**, *17*, 3189.

(5) Stewart, J. J. P. *J. Comput. Chem.* **1989**, *10*, 209, 221.

(6) For reviews, see: (a) Exner, O. *Correlation Analysis in Chemistry*; Chapman, N. B., Shorter, J., Eds.; Plenum Press: New York, 1978; Chapter 10, pp 439. (b) Charton, M. *Prog. Phys. Org. Chem.* **1981**, *13*, 119.

(7) Levitt, L. S.; Aldring, H. F. *Prog. Org. Chem.* **1976**, *12*, 119.

from its ESR spectrum that NF_3^{2+} in a solid matrix is pyramidal. The simplest analysis of their reported p/s ratio of 4.14 in terms of a C_{3v} structure with bonds pointing along the hybrid orbital directions¹² gives $\alpha(\text{av})$ of 111.3° . For comparison, AM1-UHF does properly optimize C_{3v} NF_3^{2+} as being pyramidal, obtaining $\alpha(\text{av}) = 114.6^\circ$ for the optimized structure, which is 9.7 kcal/mol lower in energy than the planar species. AM1 thus appears to calculate NF_3^{2+} to be substantially less pyramidal than it actually is, but as McBride has pointed out,¹³ the ESR measurement determines the angles of the orbital hybrids at the nucleus, which is not the same as the YXY bond angle, because of the prevalence of bent bonds in radicals. We expect steric interactions between the rather large fluorine atoms to force the FNF bond angle to be larger than that of the orbital hybrids, and therefore we expect the FNF angle to be larger than the value obtained from the ESR spectrum, although we have not tried to estimate how much larger. Symons and co-workers¹⁴ have argued for planar $\text{R}_2\text{NCl}^{2+}$ structures from their matrix ESR spectra of examples with $\text{R}_2 = \text{Me, Me}$; $(\text{CH}_2)_4$; and $(\text{CH}_2)_5$. Even if 1-X^{2+} species are not exactly planar at equilibrium, it seems likely that their inversion barriers are low enough that Figure 1 (which assumes planar nitrogen atoms both for the nitrogen inversion transition state and the radical cation) can be used without introducing significant error.

As shown in Figure 1, the changes in $a\text{IP}$ should reflect those in ΔG_e^\ddagger , except for solvent effects. The values of $\delta a\text{IP}$ calculated by AM1 are given in Table IV. We also note that $a\text{IP}$ can be dissected into nitrogen inversion (ΔH_i^\ddagger) and nearly vertical planar haloamine ionization (ΔH_e^\ddagger) components, in the same way as shown on the solution side of the diagram. We use ΔH instead of ΔG values to denote the changes on the gas side because entropies have not been calculated, so only enthalpies are available, and because ionization potentials are also enthalpies, not free energies. Calculated changes in the components of $a\text{IP}$ are shown on the last two lines of Table III. Use of the calculated $\delta a\text{IP}$ values as an approximation to $\delta\Delta G_e^\ddagger$ in eq 3 produces estimated $\delta\Delta G_i^\ddagger$ values of +0.6 (1-Br) and -3.3 (1-I) kcal/mol. Although the sign of $\delta\Delta G_i^\ddagger$ is still wrong, the experimental values being -0.5 (1-Br) and ca. -6.5 (1-I) kcal/mol, comparison with experiment is clearly much better with use of the calculated $a\text{IP}$ changes than either the experimental or the calculated $v\text{IP}$ values. We note that the fact that AM1 calculations do not correctly reproduce the changes in nitrogen inversion barriers as the halogens are changed makes it unlikely that it could calculate the changes in ease of electron removal from the planar forms properly either. Calculation of $\delta\Delta H_e^\ddagger$ values with $\delta\Delta H_e^\ddagger = \Delta H_f(\text{cation}) - \Delta H_f(\text{neutral optimized with planar nitrogen atom})$ gives values of +2.2 (1-Br) and +3.4 (1-I), use of which in eq 3 leads to estimated $\delta\Delta G_i^\ddagger$ values of -5.0 (1-Br) and -11.9 (1-I), which are of course far too negative, just as the calculated $\delta\Delta H_i^\ddagger$ values are.

Independently of how well calculations might or might not work, the $\delta\Delta G_e^\ddagger$ values determined by CV measurements and $\delta\Delta G_i^\ddagger$ values from dynamic NMR measurements allow estimation of $\delta\Delta G_e^\ddagger$ values, e.g. how much easier it is to remove an electron from the planar transition state for nitrogen inversion, including solvent effects, than it is from the reference compound, 1-Cl (using eq 3). We include these numbers in Table IV and compare them with those for the nitroxide 1-O $^\bullet$, and the *tert*-butyl and methyl amines, 1-*t*-Bu and 1-Me (their CV and PE data are from ref 2). Figure 1 is also applicable to these derivatives of 1 because their third substituents at nitrogen have 3-fold or higher symmetry. Experimental inversion barriers are not available for 1-O $^\bullet$ or 1-*t*-Bu, but both are certainly slightly pyramidal at N. The nitroxide inversion barrier is probably under 2 kcal/mol,¹ and the 1-*t*-Bu barrier is likely to be slightly higher than the 3.1 kcal/mol calculated by AM1 (several trialkylamine barriers are calculated

to be too low)⁸ but significantly less than that of 1-Me; the 4 \pm 1 kcal/mol used in Table IV seems to be a reasonable range. The $E^{\circ'}$ is not available for 1-Me, and the numbers in curly brackets in Table IV use the E_p^{ox} value. If rapid radical cation decomposition shifted E_p^{ox} to a value more negative than $E^{\circ'}$, which is the expected direction of the deviation, this would result in a less negative value of $\delta\Delta G_e^\ddagger$ corresponding to 2.3 kcal/mol for each 100 mV of kinetic shift. Because we would expect $\delta\Delta G_e^\ddagger$ to be rather similar for 1-Me and 1-*t*-Bu (the *tert*-butyl group should stabilize the cation radical center slightly better than a methyl group, but decreased solvent stabilization because of the bulkier substituent is likely to cancel this effect, and possibly lead to a less negative value of $\delta\Delta G_e^\ddagger$ for the *tert*-butyl compound),¹⁰ we doubt that E_p^{ox} is far from $E^{\circ'}$ for 1-Me. It will be noted that changes in ease of electron removal from the planar form in solution are far smaller than changes in gas-phase $v\text{IP}$ for these compounds, the total range for substituents from Cl to Me being under 10 kcal/mol in solution, while that for $v\text{IP}$ is about three times as great. Solvent effects appear to be significant, although we cannot separate the solvation component from the rest of $\delta\Delta G_e^\ddagger$ from our data.

Conclusion

The ca. 0.5 and 6.5 kcal/mol lower inversion barriers observed for 1-Br and 1-I than for 1-Cl indicate that electron removal from the planar bromide and iodide is about 2.3 and 2.0 kcal/mol easier than from the chloride in solution. The change in ease of oxidation in solution from planar nitrogen atom forms of 1-X from X = Cl to other halogens, O $^\bullet$, and alkyl varies from about 18 to 60% that for $v\text{IP}$. Semiempirical AM1 calculations do a rather good job on changes in $v\text{IP}$ for 1-X, but they overestimate the lowering of the nitrogen inversion barrier as Cl is replaced by heavier halogen atoms. We are unable to comment usefully on how large solvation energy differences between 1-Cl $^{2+}$ compounds might actually be.

Experimental Section

9-Fluoro-9-azabicyclo[3.3.1]nonane (1-F). A solution of 1-HCl (0.900 g, 5.57 mmol) dissolved in 10 mL of 15% Na_2CO_3 was extracted with ether (3×25 mL), and the combined organic phase was placed in a 3-necked flask equipped with a reflux condenser and a gas dispersion inlet tube. A solution of 0.5 g of NaOH dissolved in 30 mL of H_2O was added to the flask, and FClO_3 was slowly bubbled through the solution for 10 min. The resulting cloudy solution was deaerated with N_2 for 20 min. The organic phase was separated, washed with H_2O (30 mL), 10% NaOH solution (30 mL), and additional H_2O (30 mL), dried (MgSO_4), and concentrated to yield 0.2 g (35%) of 1-F as a thick yellow oil. HR MS: 143.1107 (calc), 143.1110 (found).

9-Bromo-9-azabicyclo[3.3.1]nonane (1-Br). A solution of 1-HCl (0.500 g, 3.10 mmol) dissolved in 10 mL of 15% aqueous Na_2CO_3 was extracted with ether (3×25 mL) and the combined organic phases were placed in a flask containing an additional 10 mL of the Na_2CO_3 solution and cooled to 0 $^\circ\text{C}$. A solution of 0.33 g (1.85 mmol) of *N*-bromosuccinimide (Aldrich) dissolved in 50 mL of CH_2Cl_2 was added to the chilled solution over 2 h time. The solution was warmed to room temperature, and the separated organic phase was washed with H_2O (25 mL), dried (MgSO_4), and concentrated to give 0.29 g (77%) of 1-Br as a yellow oil. HR MS: 203.0307 (calc), 203.0291 (found).

9-Iodo-9-azabicyclo[3.3.1]nonane (1-I). With use of essentially the identical procedure as noted for 1-Br (except that the amine was added to a cooled solution of the halosuccinimide), 0.315 g (1.95 mmol) of 1-HCl and 0.438 g (1.95 mmol) of *N*-iodosuccinimide (Aldrich) yielded 0.287 g (58%) of 1-I as a dark red waxy solid, mp 119–120 $^\circ\text{C}$. HR MS: 251.0176 (calc), 251.0173 (found).

Cyclic voltammetry employed PAR equipment, as previously described.¹⁵ The VT ^{13}C NMR study on 1-Br employed a Varian XL-100 spectrometer and data were handled as previously described,¹⁶ and the low-temperature experiment on 1-I used a Bruker AM-500. The PES experiments used a Varian IEE-15 instrument as previously described.¹⁰

Acknowledgment. We thank the National Science Foundation (CHE-8401836 and CHE-8801588) and the National Institutes of Health (GM-29549) for partial financial support of this work.

(12) Atkins, P. W.; Symons, M. C. R. *The Structure of Inorganic Radicals*; Elsevier: Amsterdam, 1967.

(13) (a) Reichel, C. L.; McBride, J. M. *J. Am. Chem. Soc.* **1977**, *99*, 6758. (b) McBride, J. M. *J. Am. Chem. Soc.* **1977**, *99*, 6760.

(14) Chandra, H.; Bathgate, A.; Malpass, J. R.; Moss, R. E.; Symons, M. C. R. *J. Chem. Soc., Perkin Trans. II* **1988**, 1329.

(15) Neisen, S. F.; Willi, M. R.; Mellor, J. M.; Smith, N. M. *J. Org. Chem.* **1986**, *51*, 2081.

(16) Neisen, S. F.; Gannett, P. M. *J. Am. Chem. Soc.* **1981**, *103*, 3300.

(17) Neisen, S. F.; Rumack, D. T.; Meot-Ner(Mautner), M. *J. Am. Chem. Soc.* **1988**, *110*, 7945.